

# Lithium and Cesium Doping on the Properties of ZTS Crystals (Tris (Thiourea) Zinc (II) Sulphate)

**Dr. P. Girija**

Assistant Professor, Department of chemistry, Annamalai University, Annamalainagar-608002, India.

## Abstract

The influence of alkali metals (Cs and Li) doping on the properties and crystal growth of tris(thiourea)zinc(II)sulphate crystals by slow evaporation solution growth technique at 30°C has been investigated. Each metals as dopant incorporate into the crystal lattice even at its low concentrations is well confirmed by energy dispersive X – ray spectroscopy (EDS). In the powder X –ray diffraction (XRD), high intense peaks are observed for all doped specimens due to stress developed in the crystal because of doping when compared to pure one. Single crystal XRD reveals a nominal increase in the cell parameter values of the doped samples compared to pure. Presence of each alkali metal (Li, Cs) quantitatively is confirmed by inductively coupled plasma (ICP) technique. It is interesting to observe the enhancement of fluorescence intensity of pure ZTS by the dopant in the photoluminescence (PL) spectra. The grown crystals are also characterized by FT-IR, UV-Visible and TG/DSC methods. The second harmonic generation (SHG) efficiency, an essential character required for the single crystals to identify the non-linear optical (NLO) property, was performed by kurtz powder technique.

**Keyword:** Alkali metals, Band gap energy, SHG, ICP.

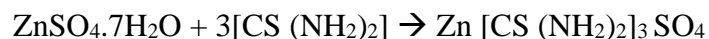
## Introduction

Recent fact reveals that doping influences the electrical, mechanical, electrooptical properties, also the nature of host material and the dopant is influenced by their surface morphology [1-13]. A promising semiorganic NLO material is suitable for Nd:YAG laser with high SHG efficiency laser damage threshold. Its SHG and laser damage threshold values are 1.2 [14] times that of KDP [15]. Being a good engineering materials for SHG device application and laser fusion experiments, with a novel metal organic crystal with potential application in electro-optic modulation, ZTS belongs to orthorhombic system with the space group Pca2, (point group mm2 ) though the crystal growth, kinetics and characterization of ZTS are reported [16-20], the effect of alkali metals doping (1 mol%) in the growth medium of ZTS single crystals systematically has not been reported. This made me an interest in this area. This paper explains the doping effect of alkali metals like lithium and cesium(1mol%) to Tris thiourea zinc sulphate through FTIR, UV-VISIBLE SPECTR, POWER XRD, SEM-EDS, SINGLE CRYSTAL XRD, ICP, PL SPECTRA, TGDSC AND SHG.

## Experimental

### Synthesis and crystal growth

Zinc sulphate heptahydrate (EM) and thiourea (SQ) are mixed in 1:3 stoichiometric ratio to synthesise tris(thiourea)zinc(II)sulphate (ZTS) as given in the chemical reaction. During preparation in the deionized water, (<70°C) temperature was maintained.



Re-crystallization was repeated in order to purify the product. Crystal growth was performed by a slow evaporation solution growth technique (SEST). A saturated aqueous solution of ZTS was prepared. The alkali metals Li (I) in the form of Li, CO<sub>3</sub>, Cs (I) in the form of CsCl are mixed as impurity in 1 mol% concentrations to the aqueous growth medium. The seed crystals floats on the saturated solution and left for slow evaporation at room temperature (30°C). Solvent used is triply distilled water. Within 15-20 days the crystallization took place and when they attained an optimal size and shape they were harvested. High quality transparent crystals were harvested from the growth medium at low concentration (1 mol%) of dopants. Photographs of the as-grown doped and undoped crystals are shown in fig. 1.

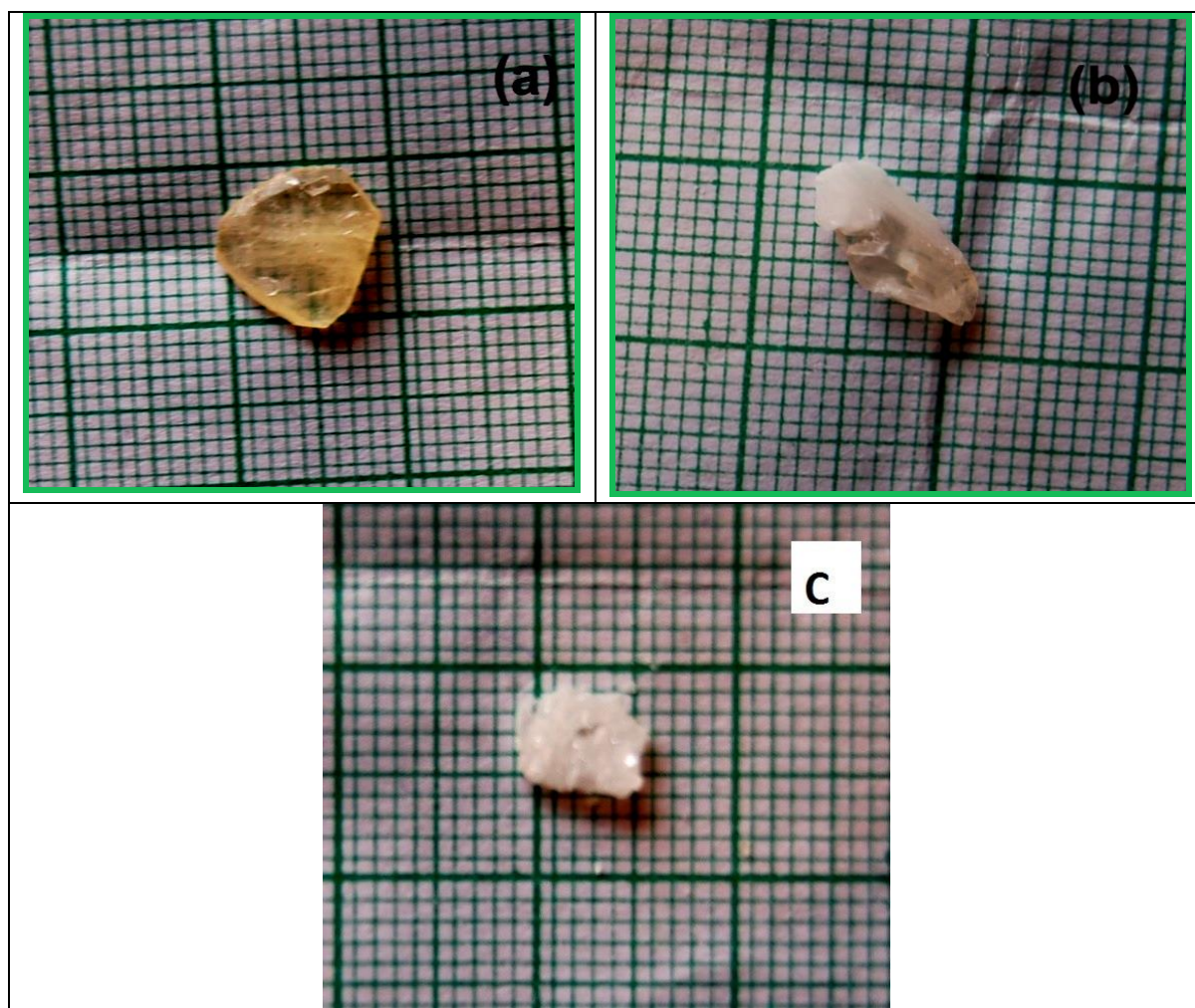


**Figure 1** Images of (a) Pure ZTS, (b) ZTS Li and (c) ZTS Cs doped crystals

## Materials and Methods

### FT-IR:

A comparison of FT-IR spectra of pure and doped ZTS specimens reveals that the doping results in small shifts in some of the characteristic vibrational frequencies, which could be due to lattice strain developed as a result of doping. An absorption band in the region  $2750$  to  $3400\text{cm}^{-1}$  corresponds to the symmetric and asymmetric stretching frequencies of  $\text{NH}_2$  group. The absorption bands observed in the spectra of pure ( $1624\text{ cm}^{-1}$ ) and doped specimens ( $1627\text{ cm}^{-1}$  for Li (I),  $1631\text{ cm}^{-1}$  for Cs(I) respectively) correspond to that of ( $1126.93$  and  $1513.14\text{ cm}^{-1}$ ), Cs(I)-doped ZTS ( $1122$  and  $1508\text{ cm}^{-1}$ ). The CS stretching frequencies of thiourea ( $1417$  and  $740\text{ cm}^{-1}$ ) are shifted to lower frequencies for pure ( $1398$  and  $712\text{ cm}^{-1}$ ), Li(I)-doped ( $1400$  and  $716\text{ cm}^{-1}$ ), CS(I) doped ( $1399$  and  $715\text{ cm}^{-1}$ ) from the above observation we can suggest that the alkali metals (Li,Cs) co-ordinate with thiourea through sulfur only.

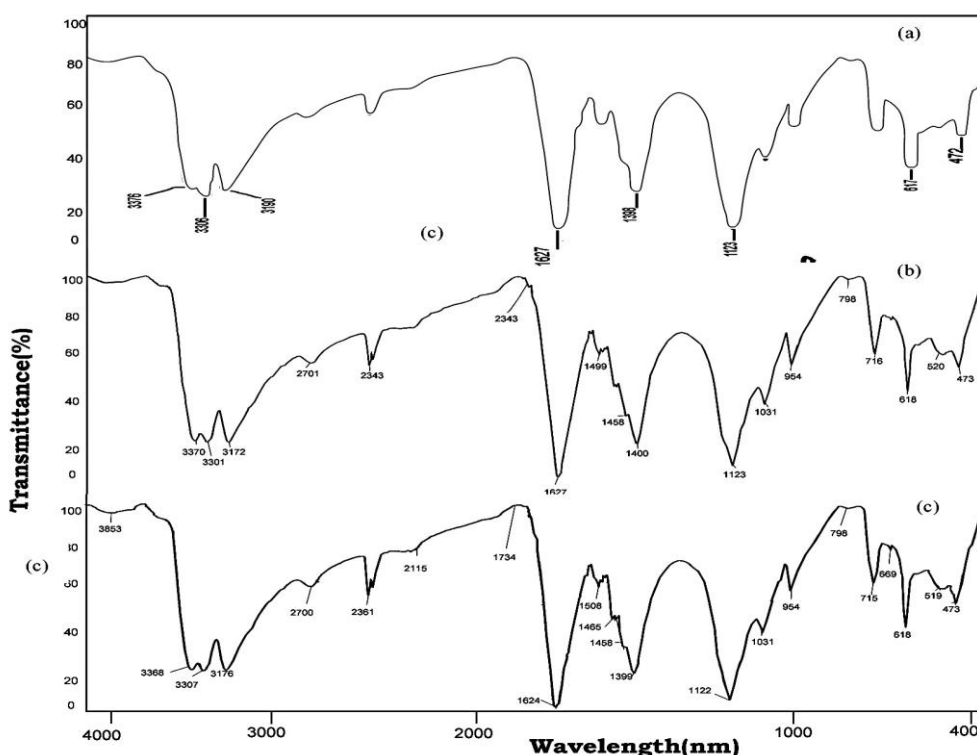


Figure 2 FTIR of (a) Pure ZTS, (b) ZTS/Li, (c) ZTS/Cs doped crystals.

### Powder and single crystal XRD analyses:

The powder XRD patterns of pure and alkali metals (Li, Cs) doped-ZTS specimens are shown in fig. 3. It reveals that the no new phases were observed by doping, however there are changes in the intensities of some characteristic peaks. In the case of Li(I) and Cs (I)-doped ZTS multi peaks are obtained with low intensity when compared to pure ZTS. The most prominent peaks with maximum intensity of the XRD patterns of pure and doped specimens are quite different. The undoped and doped specimens belong to orthorhombic system with  $P_{ca}2_1$  space group. These attributed to strains in the lattice. From the schereer equation the particle size of samples is calculated as Li(I)-  $14.49\text{ nm}$  and CS (I)-  $12.61\text{nm}$ , the single crystal XRD values for alkali metal (Li, Cs) doped ZTS crystals vary only slightly from that of pure ZTS, which is given in the Table 1. **JCPDS value of ZTS**

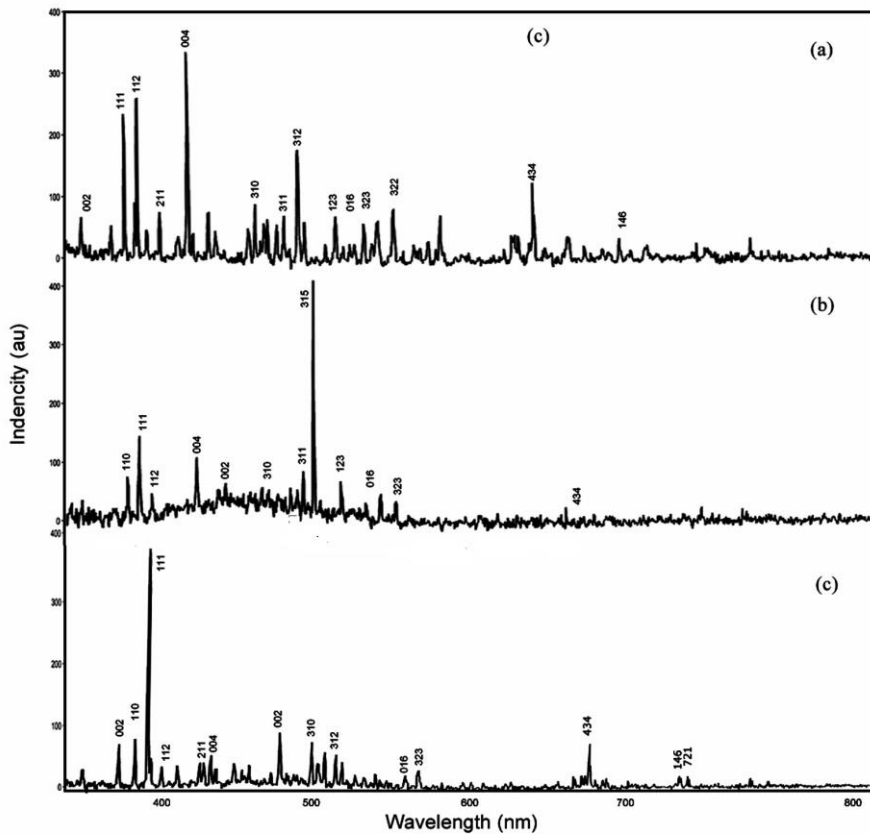
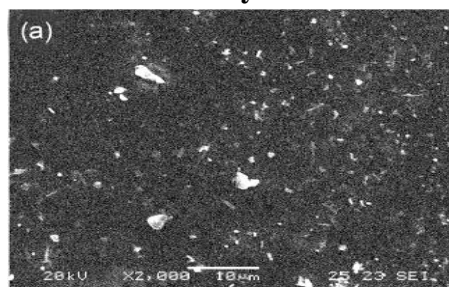


Figure.3 Powder XRD (a) Pure ZTS, (b) ZTS/Li, (c) ZTS/Cs doped crystals

Table 1. JCPDS value of ZTS

System	a Å	b Å	c Å	v Å <sup>3</sup>	Space Group and System
ZTS	7.794	11.152	15.494	1348	orthorhombic system with P <sub>ca</sub> 2 <sub>1</sub>
ZTS-Li	7.807	11.157	15.508	1339	orthorhombic system with P <sub>ca</sub> 2 <sub>1</sub>
ZTS-Cs	7.768	11.113	15.461	1338	orthorhombic system with P <sub>ca</sub> 2 <sub>1</sub>

SEM-EDS Analysis



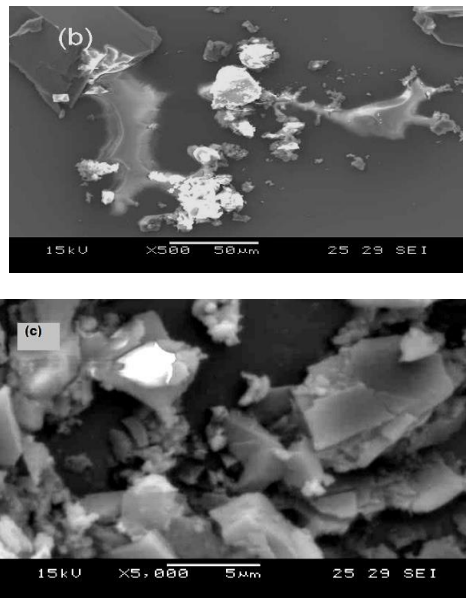


Figure 4 SEM – EDS of (a) Pure ZTS, (b) ZTS/Li, (c) ZTS/Cs doped crystals

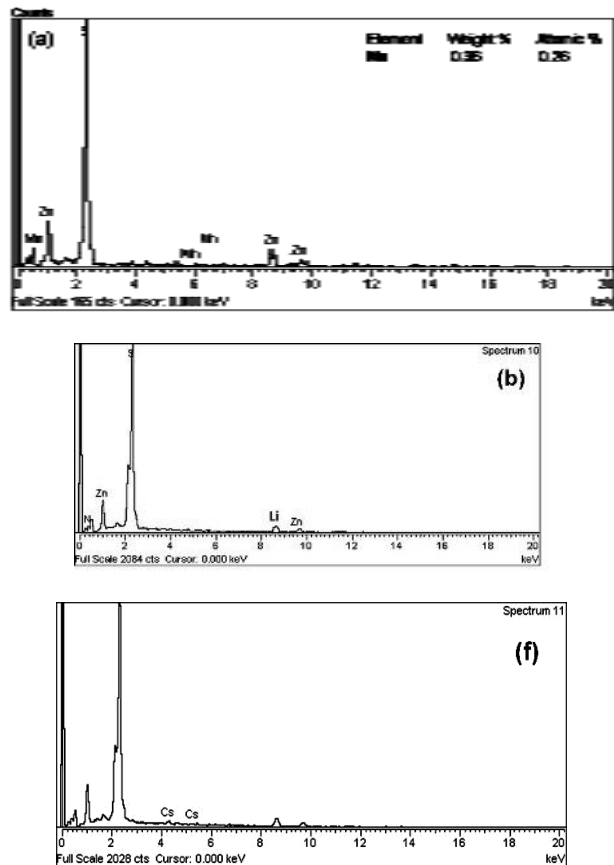


Figure 4 SEM – EDS of (a) Pure ZTS, (b) ZTS/Li, (c) ZTS/Cs doped crystals

The information about the surface nature and its suitability for device fabrication is given by SEM study. Also the presence of the influence of alkali metals (Li, Cs) doping on the surface morphology of ZTS crystal reveals the formation of structure defect centers. In the case of Li(I) doped ZTS, larger scatter centers are observed. Cs(I) doped ZTS shows cauliflower like appearance as shown in fig. 4.

The EDS graph confirms the presence of the alkali metals and the incorporation of the alkali metals into the ZTS crystalline matrix which is very clear from Fig 5. Analysis of the surface at different sites reveals that the incorporation of metals is non-uniform over the whole crystal surface.

**ICP:**

The amount of dopant in alkali metals (Li,Cs) doped specimens are estimated using ICP and the foreign metal ion entering into the ZTS crystal matrix is much smaller but significant. The actual dopant concentration in the crystalline matrix is given in Table 2. Doping and actual concentrations of alkali metal (Li, Cs).

Sample	Actual dopant concentration in the crystalline matrix/ ppm
ZTS-Li	4.6
ZTS-Na	34.4
ZTS-Cs	5.8

**Optical studies:**

UV-visible spectrometer in the spectral range 400-700nm for pure and doped samples are shown in fig. 5. It appears that the doping of alkali metals (Li, Cs) does not destroy the optical transmission. The cut off wavelength is nearly 350-500nm in the case of all specimens, and there is high is percentage of transmittance in the entire visible region for pure and alkali metal (Li, Cs) doped ZTS crystals. No significant  $\lambda_{max}$  shift is observed but the absorbance is reduced drastically by doping (Table-3), where there is a slight increase in absorbance value. Due to its high transparency, these doped crystals are quite useful for optical device applications. The band gap energy can be calculated using equation

$E_g = hc/\lambda_{max}$  Where: h – plank constant, C – Velocity of light,  $E_g - 1.243 \times 10^3 / \lambda_{max}$  For pure and doped specimens band gap energy is calculated and due to doping it is interesting to see an increase in band gap energy value.

**Table 3 Cut off wavelength and band gap energy of alkali metals doped ZTS crystals**

Sample	Cut off wavelength (nm)	Band gap energy (ev)
ZTS	460	2.70
ZTS/Li	390	3.19
ZTS/Cs	380	3.27

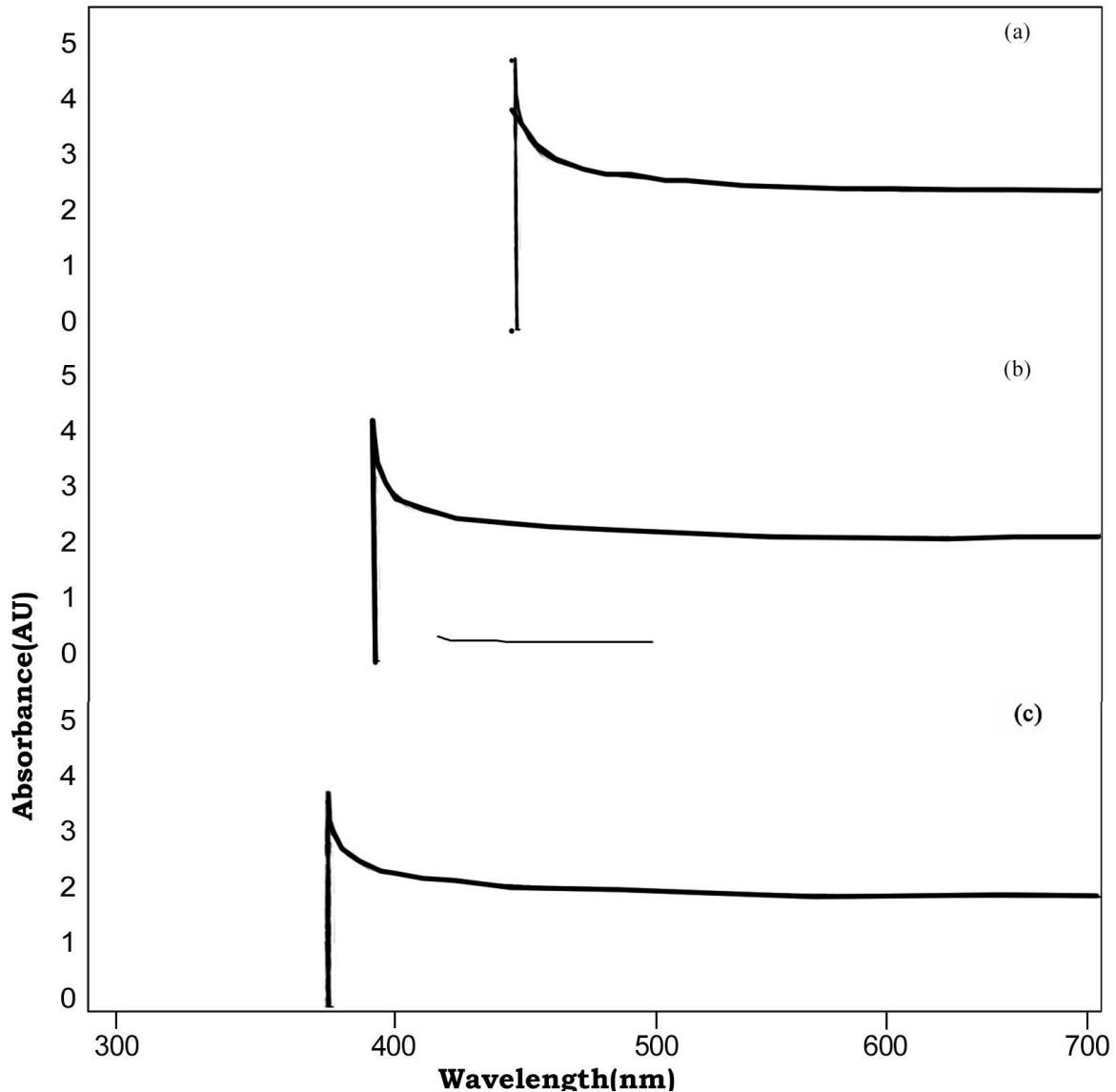


Figure 5 UV-visible of (a) Pure ZTS, (b) ZTS/Li, (c) ZTS/Cs doped crystal

### SHG

The influence of doping alkali metals (Li, Cs) on the NLO properties of the as grown ZTS and alkali metal doped ZTS crystals were subjected to SHG test with 2.5 mj/pulse as input radiation. The Table - 4 gives the output SHG intensities of pure and doped specimens from the SHG values it is clear that in the case of doped Li(I) specimen the value is reduced than the undoped which could be due to ineffective facilitation of charge transfer by the dopant in the ZTS crystal. SHG output for Cs(I) doped specimen is greater (~1.5 times) than ZTS crystals.

Table- 4 SHG output

System	I <sub>2</sub> w/mv
Pure 2TS	6.7
2TS- Li	3.7
2TS- Cs	9.0

### PL spectral studies

The fluorescence spectra of ZTS and alkali metals doped ZTS crystals are given in the figure – 6. In the case of pure ZTS there is no fluorescence intensity but Li(I) doped ZTS crystals shows the increased peak intensity at (781.91) and Cs(I) (757.88) which are slightly lower than Li(I) doped specimen.

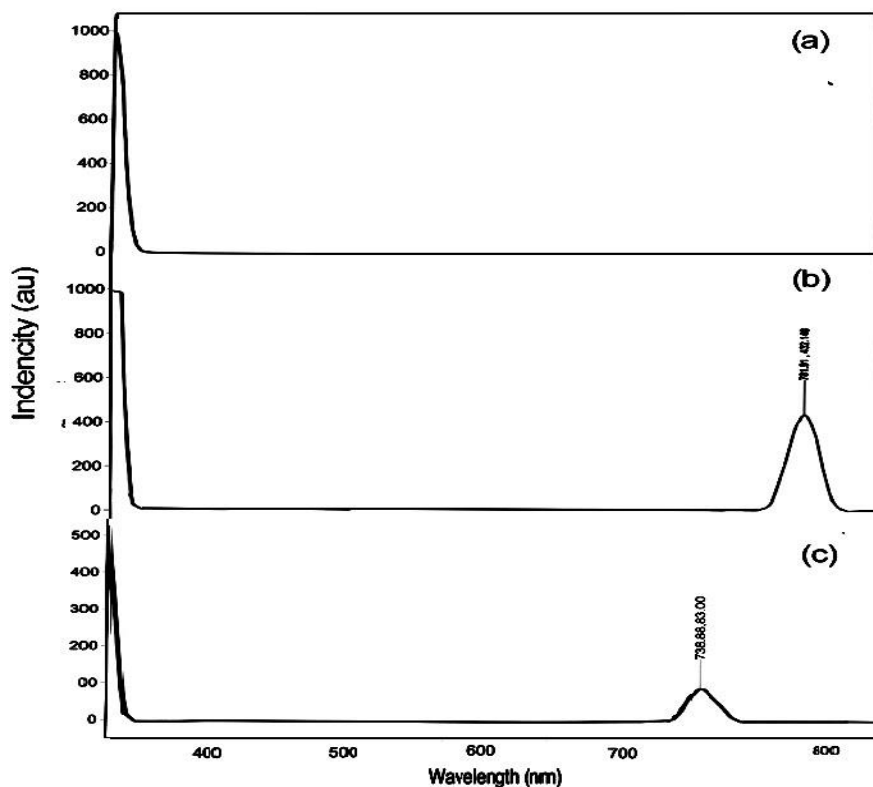
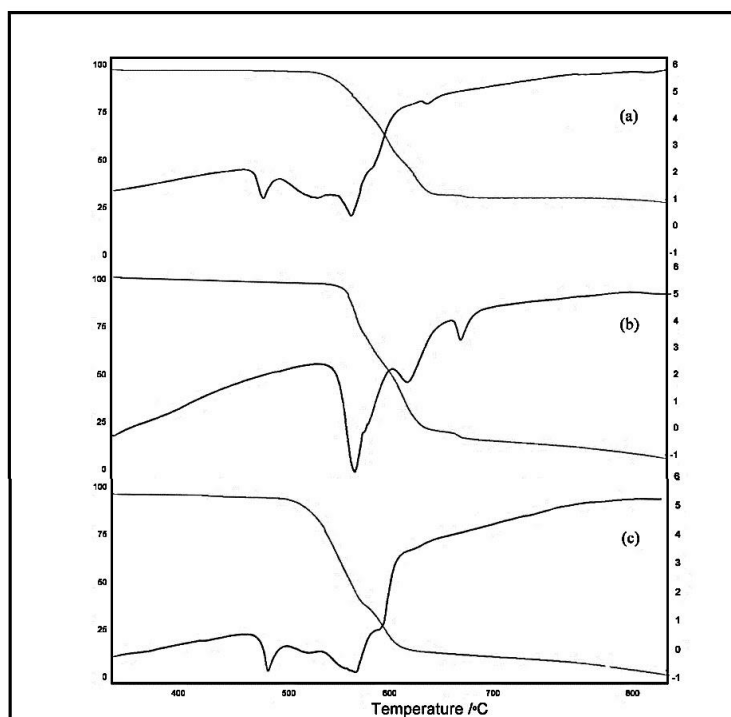


Figure 6 PL-Spectra of (a) Pure ZTS, (b) ZTS/Li, (c) ZTS/Cs doped crystals

### TG – DSC studies :-

The TG – DSC curve is recorded for pure and alkali metals Lithium and Cesium (1 mole %) doped ZTS crystal and shown in figure – 7. The absence of weight loss around 100°C shows that there is no water of hydration in the molecular structure. In the case of doped specimens the melting point is changed slightly which implies the incorporation of dopants in ZTS crystal. The suitability of the material for application in lasers is due to no de-composition up to the melting point, this implies that the materials are required for with standing high temperatures.

In DSC curve the decomposition is recorded from 10°C to 500°C. In the DSC curve, the endothermic peak at ~180°C in the figure for all doped specimens except Li(I) doped which could be due to liberation of water molecules. The three sharp endothermic peaks at 240°C – 360°C in all specimens may be due to the decomposition of alkali metals doped ZTS crystal into fragments and their subsequent volatilization.



**Figure 7 TG-DSC of (a) Pure ZTS, (b) ZTS/Li and (c) ZTS/Cs doped crystals**

## Conclusion

Transparent crystals of pure and alkali metals Li(I) and Cs(I) doped ZTS crystals are grown by slow evaporation solution grown technique. The single crystal XRD analysis gives the slight changes in all parameter value than the parent which tells that alkali metals (Li,Cs) are incorporated as dopant only in crystal matrix is evidenced by energy dispersive X – ray spectroscopy. Some minor structural variations in FT – IR and XRD is observed due to doping changes in the external morphology of metal thiourea crystal is observed due to doping in SEM images. Thermal studies reveals the purity of the material and no decomposition is observed up to the melting point. SHG reveals that there is slight decrease in the case of Li and increased enhancement in Cs compared to pure ZTS values. There is reduction in the wavelength in the case of alkali metals doped specimens compared to ZTS except Na(I) doped specimen where there is a slight increased value. PL spectra shows that there is an increased fluorescence intensity.

## References:

1. S. Meenakshisundaram, S. Parthiban, N. Sarathi, R.Kalavathy and G.Bhagavannarayana, J. Cryst. Growth, 2006, 293, 376-381.
2. G. Bhagavannarayana, S. Parthiban and S. Meenakshisundaram, J.Appl. Crystallogr., 2006, 39, 784-790.
3. G. Bhagavannarayana, S. Parthiban and Subbiah Meenakshisundaram, Cryst. Growth Des., 2008, 8, 446-451.
4. G. Bhagavannarayana, S. Parthiban, C. Chandrasekaran and Subbiah Meenashisundaram, CrystEngComm, 2009, 11, 1635, DOI: 10.1039/b904220b.
5. S.P. Meenakshisundaram, S. Parthiban, G.Madhuramambal, R.Dhanesekaran and S.C Mojumdar, J.Therm. Anal. Calorim., 2008,94,15-20.

6. G.Bhagavannarayana, S.K.Kushwaha, S.Parthiban, G.Ajitha and Subbiah Meenakshisundaram, J. Cryst. Growth, 2008, 310, 2575-2583.
7. G. Bhagavannarayana, S. K. Kushwaha, S.Parthiban and Subbiah Meenakshisundaram, J. Cryst. Growth, 2009, 311, 960-965.
8. D.Donkova, J.Pencheva and M.Djarova, Cryst. Res. Technol., 2004, 39,207-213.
9. W.S. Yang, J. H. Lee, T.Fukuda and D.H.Yoon, Cryst. Res. Technol., 2001, 36, 519-525.
10. H. E. Shall, M. M. Rashad and E. A. Abdel-Aal, Cryst. Res. Technol., 2002, 37, 1264-1273.
11. K.Sangwal, Prog. Cryst. Growth charact. Mater., 1996, 32, 3-43.
12. G. Bhagavannaryana, R. V. Ananthamurthy, G.C. Budakoti, B. Kumar and K. S. Bartwal, J. Appl. Crystallogr., 2005, 38, 768-771.
13. S. Xun, F. Youjun, G. Zhangshou, W. Shengalai, Z. Hong and L. Yiping, Chin. Sci. Bull., 2001, 46, 1142-1144.
14. H.O. Marcy, L.F. Warren, M.S. Weeb, C.A. Ebbbers, S.P. Velsko, G.C. Kennady, G.C. Catella, Appl. Opt. 31 (1992) 5051.
15. S.S Gupte, R.D. Pradhan, O.A. Marcano, N. Medikechi, C.F. Desai, J.Appl. Phys. 91 (2002) 3125.
16. P. M. Ushasree, R. Muralidharan, R. Jayavel and P. Ramasamy, J. Cryst. Growth, 210 (2000) 741.
17. Rockwell International Corporation, Seal beach, CA, Patent-US5581010: Semi-organic crystal for non linear optional devices.
18. V. Venkataramanan, G.Dhanaraj, W. K. Wadhavan, J.N. Sherwood and H. L. Bhat, J. Cryst. Growth, 154 (1995) 92.
19. P.R. Newman, L.F. Warren, L.F. Warren, P.Cunnigham, T. Y. Chang, D. E. Copper, G. L. Burdge, P. P, Dingles and C.K. Lowema, Mater. Res. Soc. Symp. Proc., 173 (1990) 557.
20. G. Arunmozhi, G. E. Dem and G. Moorthi, Cryst. Res. Technol., 39 (2004) 408.

## 2. Concentration Effects of Manganese Sulphate on the Non-Linear Optical Properties of ADP Crystal

**P. Girija**

Department of Chemistry, Annamalai University, Annamalainagar - 608002, India.

### ABSTRACT

The characterization results of influence of various concentration of Mn (II) ion on the properties and crystalline perfection of ammoniumdihydrogenphosphate (ADP) crystal are presented. Using water as a solvent pure, 1 and 20 mol % of Mn (II) ion in the form manganese (II) sulphate added ADP crystals are prepared by slow evaporation solution growth technique (SEST). Well faceted grown crystals are characterised by different experimental techniques. The presence of Mn (II) in the doped specimens is confirmed by energy dispersive X-ray spectroscopy (EDS) and inductively coupled plasma (ICP) technique. High resolution X- ray diffraction (HRXRD) study of the doped samples when compared with the pure ADP crystal reveals interesting features. In the single crystal XRD studies, the dopants have not altered the lattice parameter values and the crystal system of pure ADP. Reduction in the intensity of peaks is observed in the powder XRD of all the doped samples. It is interesting to enhancement of fluorescence intensity of pure ADP by the dopants in the photoluminescence (PL) spectra. The surface morphology of the crystals is studied by scanning electron microscopy (SEM). The grown crystals are also characterized by FT-IR,

UV-Vis and TG/DTA methods. The second harmonic generation (SHG) efficiency, which is an essential character required for the single crystals to identify the nonlinear optical (NLO) property, is performed by Kurtz powder technique. Increasing in concentrations of dopant enhance the SHG efficiency of ADP crystal.

**Keywords:** Manganese, NLO material, fluorescence, HRXRD, SEST.

## INTRODUCTION

Latest studies report that Potassiumdihydrogenphosphate (KHP) and Ammoniumdihydrogenphosphate (ADP) are some of the available nonlinear optical crystals needed for laser radiation conversion in laser fusion system<sup>1</sup>. The lattice studies on the ADP crystals still attract interest because of their unique nonlinear optical, dielectric and anti-ferroelectric properties and their varied uses as electro-optic modulator, harmonic generators and paramagnetic generator<sup>2-13</sup>. ADP, being an inorganic nonlinear optical materials has made the researchers to study about its optical transparency, good susceptibility and low thermal and mechanical stability<sup>14</sup>. The enhancement of optical transmission<sup>15</sup>, effect of complexing agent<sup>16</sup>, dopant effect of KCl and Oxalic acid<sup>17</sup>. Studies have also been made about the effect of mixing of divalent and trivalent impurities on the growth, habit modification and structure of ADP<sup>18-21</sup>. Manganese is one of the metallic elements which appear in biological apatite like bone and teeth. Its important effect on the growth and development of bone has been well known<sup>22</sup>. The  $Mn^{2+}$  d-electron states act as an efficient luminescent centres.  $Mn^{2+}$  emission was red shifted from 584-600 nm<sup>23</sup>. Further because of its transparency, it may be of use in laser production in the green region based on  $3d^{54}T_1 \rightarrow ^6A_1$  transition of Mn (II)<sup>24</sup>. A good number of investigations are reported on manganese as dopants. The unusual ferromagnetic properties of manganeseorthovanadate is studied<sup>25</sup>. The magnetic properties of nano crystals of Mn doped ZnO is recently reported<sup>26</sup>. The concentration effects of Mn (II) doping on ZTS is studied<sup>27</sup>. Aiming to find new useful materials for academic and industrial use, an attempt has been made to modify the ADP crystal by the transition metal, Mn is doped in the mother solution of ADP with different concentrations. The effect of doping is studied using FT-IR, UV-Visible spectra, XRD, SEM-EDS, ICP, PL spectra and Kurtz powder SHG measurements.

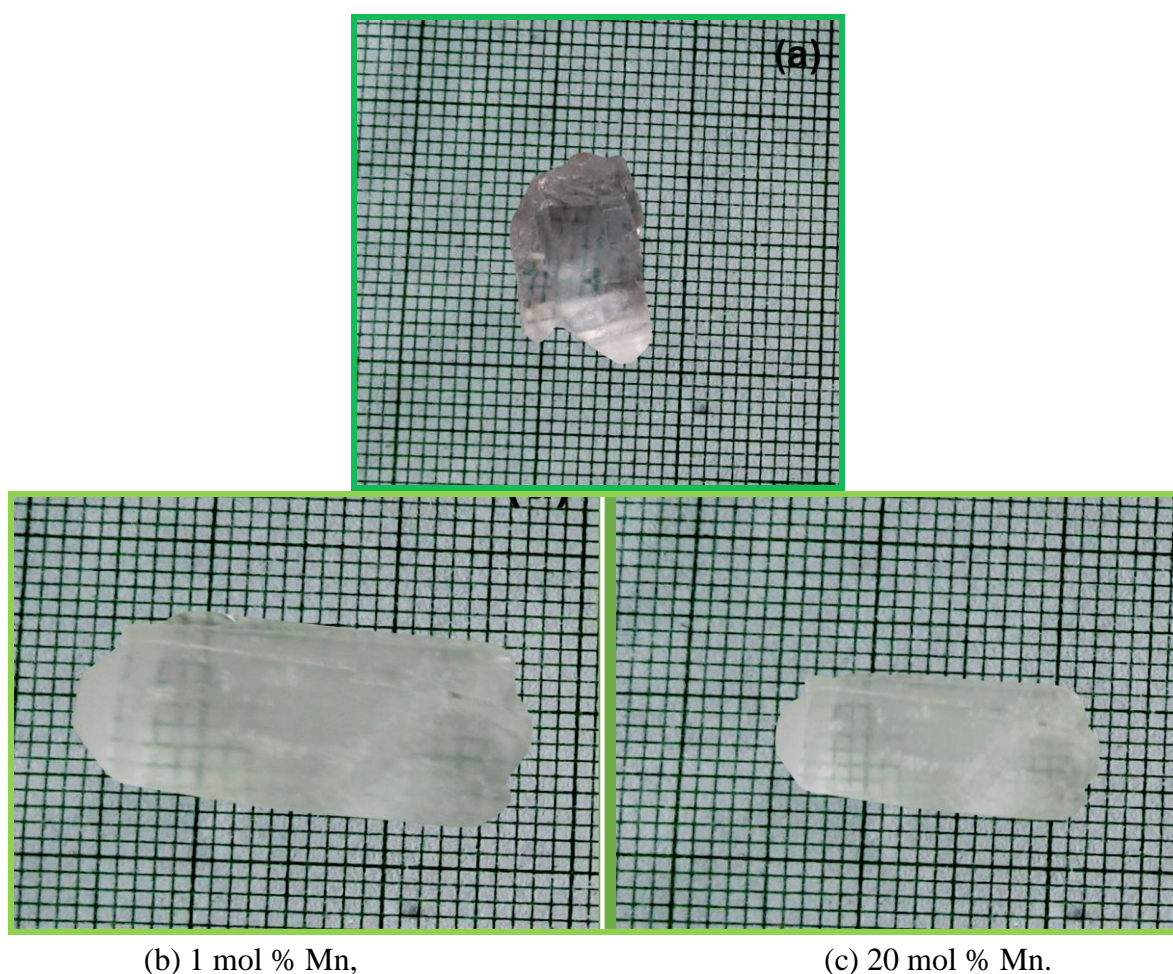
## Characterization

The FT-IR spectra are recorded using AVATAR 330 FT-IR by KBr pellet technique. The single crystal X-ray diffraction studies are performed by using the Bruker Axs (Kappa Apex II) X-ray diffractometer. UV-Visible absorption spectra is recorded in the range 300-900 nm for all samples using Hitachi. Morphologies of the samples are observed by using JEOL JSM 5610LV scanning electron microscope (SEM). EDS, a chemical microanalysis technique with cobalt as a standard, is performed in conjunction with the resolution 3.0 nm, accelerating voltage 20 kV and maximum magnification 3,00,000 times. Powder XRD is carried out by using a philips Xpert Pro Triple-axis X-ray diffractometer with Cu  $K\alpha$  radiation for  $2\theta$  ranging from  $10^\circ$  to  $70^\circ$ . Fluorescence is measured using ELICO fluorescence instrument. ICP studies are recorded using a varicun cary 5E UV-Vis-NIR spectrophotometer. The SHG efficiency of the specimens is measured by the Kurtz power method<sup>28</sup>.

## EXPERIMENTAL PROCEDURE

### Crystal Growth

Crystal growth of pure ADP is done by solution growth technique at room temperature. Analytical grade ADP has been re-crystallized thrice to extract pure ADP. Crystal growth of pure ADP is done by solution growth technique at room temperature. Different concentration of dopants viz., 1 and 20 mol % of  $\text{MnSO}_4$  are used in growth medium, and the photographs of pure and Mn-doped crystals are shown in Figure-1. The grown crystals are subjected to various characterization techniques which are briefly described below.



(b) 1 mol % Mn,

(c) 20 mol % Mn.

**Figure 1** Photographs of the doped ADP Crystals are (a) ADP Pure

## RESULTS AND DISCUSSION

### FT - IR Analysis

The Fourier transform infrared (FT-IR) investigations are carried out on the powdered samples Mn-doped ADP crystals. Figure 2 shows the prominent peaks in the FT-IR pattern Mangesesulphate doped ADP. The growth frequency region is located below  $4000$  to  $1300\text{ cm}^{-1}$  and the fingerprint region  $1300$  to  $630\text{ cm}^{-1}$ . In the spectrum 1, 20 mol% of  $\text{MnSO}_4$  doped ADP, there is a

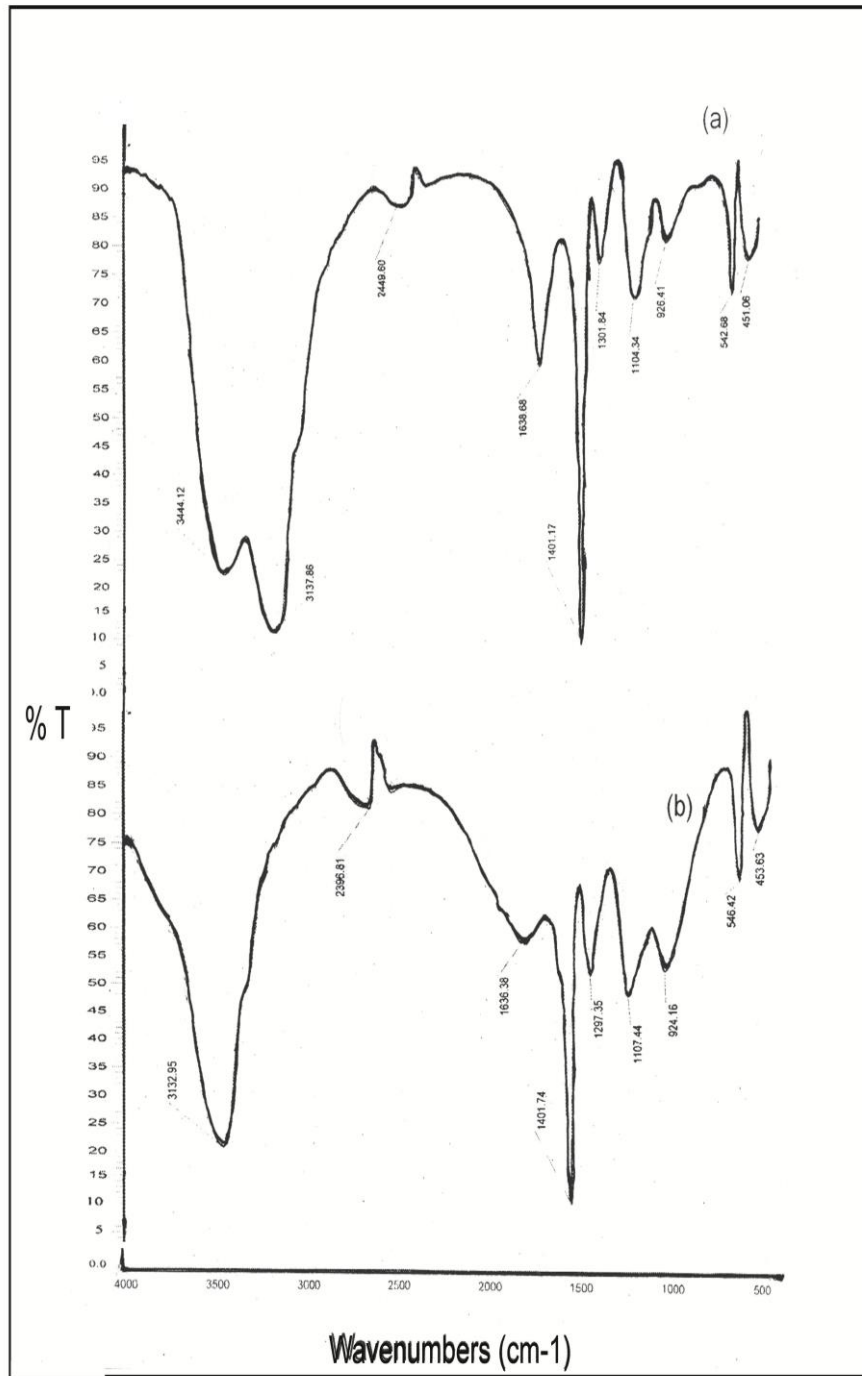


**Figure 2** FT-IR spectra of (a) ADP Pure, (b) 1 mol % Mn, (c) 20 mol % Mn doped crystals.

broadband in the higher energy region  $3100$  to  $3150\text{ cm}^{-1}$  due to O-H stretching vibration of ADP and water. In one mol% there is a broad band and a doublet appear in the region  $3100$  to  $3500\text{ cm}^{-1}$  and this may be due to hydrogen bonding within the crystal. Presence of water is supported by its bending vibrations occurring at the band  $1642.93\text{ cm}^{-1}$  for pure ADP, but in the case of Mn-dopants the broadband is narrowed due to the doping effect. The absorption at  $1642.93\text{ cm}^{-1}$  is assigned to C = O stretching of COOH group. The intensity of the peak for Mn-doped ADP is very sharp in the range  $1401$

to  $1401.74\text{ cm}^{-1}$  and this is due to the incorporation of Mn on the lone pair of ammonia and the absence of hydrogen bonding.

### UV-Visible Spectra

UV-Visible spectrometer in the spectral range 200-1000 nm for pure and doped samples are shown Figure 3. The optical transmissions are not altered much in the case of Mn (II) doping. The cut off wavelength is nearly 350-400 nm in the case of all the specimens, and there is high percentage of transmittance in the entire visible region for pure and Mn-doped ADP specimens. It indicates that the dopants have not destroyed the optical transparency of the crystal.

**Figure 3** Optical transmission spectra of (a) ADP Pure, (b) 1 mol % Mn, (c) 20 mol % Mn doped crystals.

### SEM and EDS

The investigation of influence of Mn (II) doping on the surface morphology of ADP Crystal faces reveals the formation of structure defect centres<sup>29</sup>. The incorporation of manganese in the crystalline matrix results in more scatter centres than the undoped specimens in Figure 4. The presence of Mn in the doped specimen was confirmed by EDS.

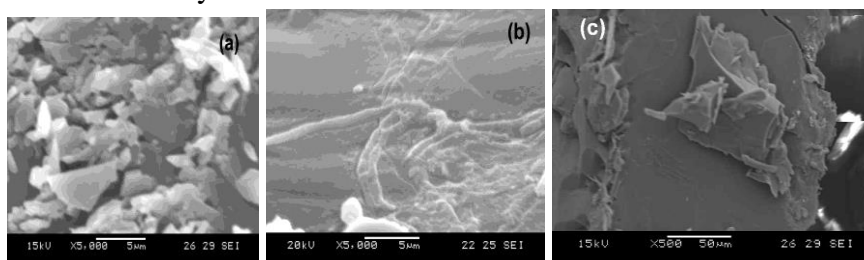


**Figure 4** SEM of (a) ADP Pure, (b) 1 mol % Mn, (c) 20 mol % Mn doped crystals.

The different concentration of the incorporation in to the ADP crystalline matrix can be clearly seen in Figure 5, i.e. the incorporation of Mn increases with higher dopant concentration in the solution except 5 mol% where the Mn incorporation is very high. The presence of Mn in the doped ADP crystals is also established by a spot test. To a drop of the test solution a portion of crystal dissolved in water on a spot plate, a drop of dilute  $\text{HNO}_3$  and then a little sodiumbismuthate are added. Development of purple colour confirms the presence of Mn.

**Figure 5** EDS graph of (a) ADP Pure, (b) 1 mol % Mn, (c) 20 mol % Mn doped crystals.

### ICP Analysis

The amount of dopant in ADP Mn specimens are estimated using ICP and the foreign metal ion entering into the ADP crystal matrix is much smaller but significant. Further, the final dopant concentration within the host lattice is not proportional to the prevailing concentration of dopant in the solution at the time of the crystallization process<sup>30</sup>, since the host crystal can accommodate the dopant only to a limited extent Table 1, the ICP results shows that there is a gradual increase in the values (ppm) on increasing the dopant concentration. The dopant metal ion entering into the ADP crystal matrix is smaller but

significant. The ADP crystals can accommodate the dopant (Mn) only to a limited extent because ADP lattice is not proportional<sup>31</sup>.

**Table 1 ICP Values for Doped ADP Crystals**

System	$I_{2\omega}$ (mV)
ADP-Mn <sup>2+</sup> 1%	15.95
ADP-Mn <sup>2+</sup> 20%	39.27

### SHG Efficiency

In order to confirm the influence of doping on the NLO properties, the as grown and doped crystals were subjected to SHG test with input radiation at 2.5 mJ/pulse. The SHG output intensities of pure and doped specimens give the relative NLO efficiencies of the measured specimens. It is clearly seen from Table 2, that doping has a significant influence on the NLO properties of ADP crystals, irrespective of the concentration of Mn.

**Table 2 SHG Values for Pure and Doped ADP Crystals**

System	$I_{2\omega}$ (mV)
ADP Pure	24.00
ADP- Mn <sup>2+</sup> 1%	51.50
ADP- Mn <sup>2+</sup> 20%	57.50

The SHG efficiency due to ineffective facilitation of charge transfer in the host crystal by the dopant which is present in the crystal at a very low level. However, there is a significant increase in the SHG value with increasing concentration of manganese doped ADP crystals.

### Thermo Gravimetric Analysis (TGDTA)

The information regarding phase transition, water of crystallization and different stages of decomposition of the crystal system is studied in TGDTA. The thermal analysis of pure and Mn-doped ADP crystals are shown in Figure 6. In TGA, for all the specimens there is no weight loss ~ 185°C indicating no inclusion of water in the crystal lattice, which is used as a solvent for crystallization.

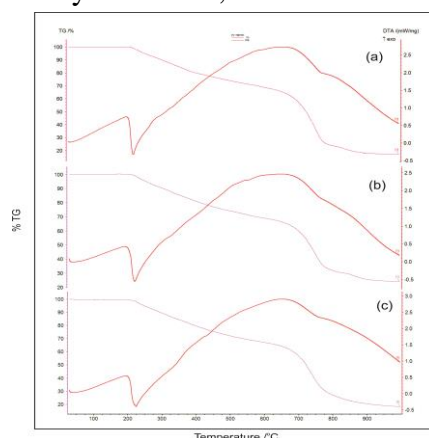


**Figure 6** TG-DTA curve of (a) pure ADP, (b) 1 mol % Mn doped ADP crystals, (c) 20 mol % Mn ADP crystals.

Major weight loss starts at ~ 220°C, indicating the decomposition point of the material. However, above this temperature, no weight loss has been observed. In DTA, the strong endothermic peaks located around 230°C show the good crystallinity of the specimens.

### Photo Luminescence Spectra

Figure 7 represents the fluorescence spectra of ADP and 1 and 20 mol % of Mn-doped ADP crystals. It is observed that doping increases the fluorescence intensities. There is blue shift that is in the wavelength region of 683.00 to 661.14 nm. Shift in emission maximum is appreciable and there is a decrease in intensities of dopant peaks when compared to pure ADP peak and so the wavelength increases. Table 3 shows the value of wave length and intensities of the peak obtained.

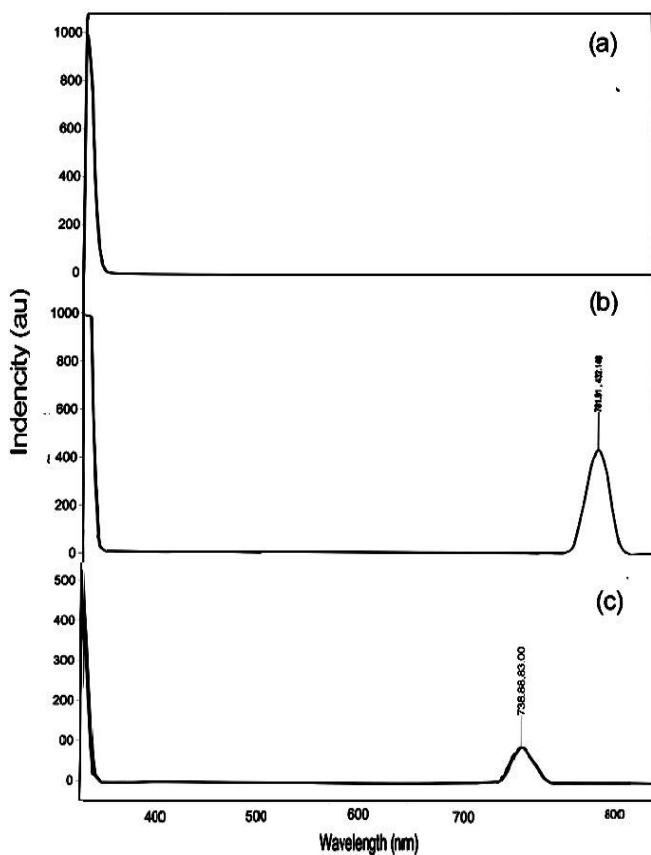


**Figure 7** PL spectra of ADP crystals (a) ADP Pure, (b) 1 mol % Mn, (c) 20 mol % Mn.

**Table 3** PL Spectra Values for Pure and Doped ADP Crystals

System	Wave Length (nm)	Intensity
ADP Pure	683.00	162.49
ADP- Mn <sup>2+</sup> 1%	661.14	138.70
ADP- Mn <sup>2+</sup> 20%	758.87	100.40

### XRD Studies

X - ray diffraction analysis of 1 and 20 mol % Mn-doped ADP crystals were carried out and their respective lattice parameter values are given in Table 4. These values are very close to corresponding JCPDS data card No (850815) values for pure ADP with very normal changes due to doping<sup>1</sup>. XRD patterns of 1, 5, 10 and 20 mol % Mn- doped ADP crystals are compared with that of pure ADP crystal in Figure 8. The Bragg's reflection is induced for pure and doped ADP crystals using the cell parameters. Comparing the intensities of the peaks of the doped one with that of the pure, it is found that generally the relative intensity is increased by doping. This could be due to the large particle size. The sizes of the samples are calculated using sherrer equation.

$$t = k \lambda / \beta \cos \Theta$$

Where:

t- Averaged dimension of crystallites,

k - Scherer constant, (it is usually assumed to be 1)

$\lambda$  - Wave length of X- ray,

$\Theta$  - Peak position measured in radian,

$\beta$  - Integral breadth of reflection (in radian  $2\Theta$ ) located at  $2\Theta$ .

The granularity of the crystal increases from 10.38 to 11.76 nm by doping. It appears that the Mn (II) doping does not inhibit the growth of the crystals. In the curve Figure 8 (a) and (b) the peak intensities of lower order reflections are very prominent and increase in the low doped specimens. The minute changes in the peak intensities, peak shifts in the observed XRD and the meagre increase in lattice parameter could be attributed to the strain developed by the incorporation of Mn in the interstitial position of the crystalline matrix as revealed in HRXRD.

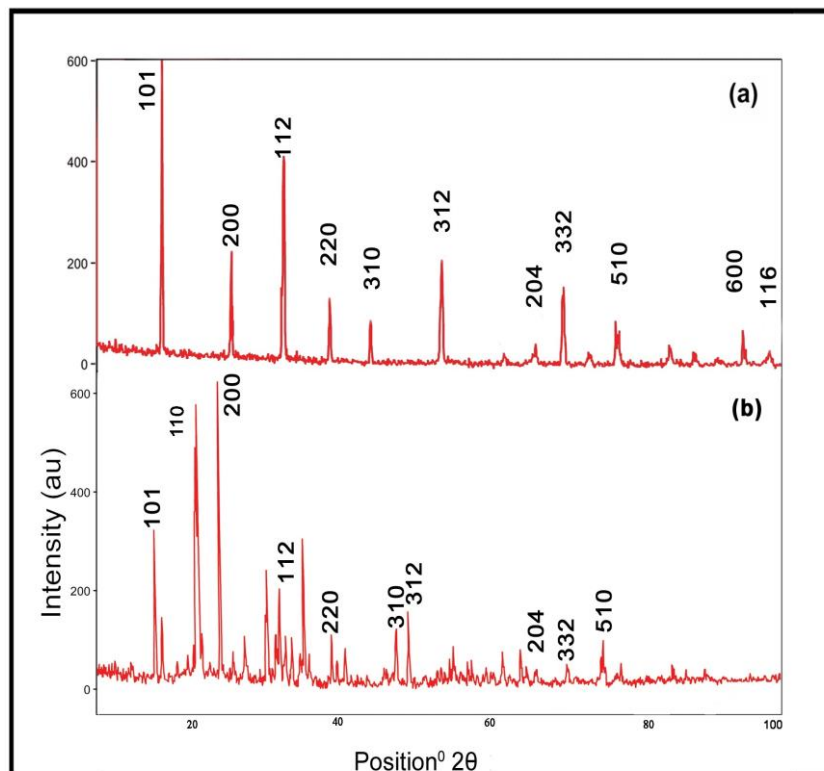


**Figure 8** Powder XRD curves of ADP crystals: (a) ADP Pure, (b) 1 mol % Mn, (c) 20 mol % Mn.

**Table 4 Single Crystal XRD Values for Pure and Doped ADP Crystals**

Property	ADP Pure	ADP- Mn <sup>2+</sup>			
		1%			20%
a	7.50	7.48			7.46
b	7.48	7.48			7.46
c	7.55	7.48			7.46
v	421. 0	422. 0			415.8

### CONCLUSION

An important role is played by the transition metal Mn as dopant in ADP crystals. Also there is an influence on the NLO properties due to the slight distortion of the crystal structure by the dopant to the host crystal. EDS and chemical analysis confirm the presence of Mn in the doped specimens. There are some minor changes in the vibrational peaks of Mn doped ADP crystals in FT-IR. A close observation of XRD profiles of doped and undoped samples reveals some minor structural variations. Changes in the intensity patterns and slight shift in peak positions are observed because of doping. Increase in concentration of Mn doping increases the value also, in the case of ICP. UV-Visible implies that the absorption is maximum for Mn-doped crystals. PL spectra shows that there is increase in fluorescence on increasing the concentration of Mn in ADP crystal. These investigations show that the crystal is under stress. SHG efficiency is improved considerably with dopant concentration.

### REFERENCES

- Jagatheesan,A.; Neelakantaprasad,B.; Murugan,J.; Rajarajan,G. Int. J comp. appl. **2012**, 53, 15-18.
- Zaitseva,N.; Carman,L. Prog. cryst. growth charact. **2001**, 43, 1-118.
- Glasser,L. Chem. Rev. **1975**, 75, 21-65.
- Gunning,M.J.; Raab,R.E.; Kucharczyk,W. J.opt.soc.Am. **2001**, 18, 1092.
- Rushton,E. Br. J.Appi.Phys.**1961**,12, 417.
- Peres,N.; Boukhis,A.; Souhassou,M.; Gavaille,G.; Lecomte,C. Acta Cryst. **1999**, 55, 1038.
- Ledzion,R.; Bondarczuk,K.; Kucharczyk,W. Cryt. Res. Technol. **2004**, 39,161.
- Galass,A.M.; Lines,M.E. Principles and Applications of Ferroelectric and Related Materials; oxford university press; oxford, **1977**; pp.293.
- Courtens,E. Helv.Phys.Acta. **1983**, 56, 705.
- Ermerl,D. Ferroelectrics. Ferroelectrics. **1987**, 72, 95.
- Zajtseva, N.P.; Bogatyreva, S.V. J. Crystal growth. **1995**, 148, 276.
- Dmitriev, V.G.; Gurzadyan,G.G.; Nikogosyan,D.N.In Hand book of nonlinear optical crystal; Berlin; Heidelberg, **1991**, pp.14-35.
- Jayarama,A.; Dharmaprakash,S.M. Applied Surface Science. **2006**, 253, 944-949.
- Wankhede,P.M.; Gundale,S.A.; Rode,M.N.; Muley,G.G. Int. J. Basic and App. Res. **2012**, special issue, 290-292.
- Bhagavannarayana,G.; Kushwaha,S.K.; Parthiban,S.; Subbiah Meenakshisundaram. J. Crystal growth. **2009**, 311, 960-965.

16. Meenakshisundaram,S.P.; Parthiban,S.; Madhurambal,G.; Dhanasekaran,R.; Mojumdar,S.C. J.Therm.Anal.Calorim. **2008**, 94, 15-20.
17. Bhagavannarayana,G.; Parthiban,S.; Subbiah Meenakshisundaram. Cryst.Growth Des. **2008**, 8, 446-451.
18. Peng,W.Q.; Qu,S.C.; CongG.W. J.crystal growth. **2005**, 279, 454.
19. Venkataramanan,V.; Dhanaraj,G.; Wadhawan,V.K.; Sherwood,J.N.; Bhat,H.L. J.crystal growth. **1995**, 154, 92.
20. Jouini,A.; Yoshikawa,A.; Fukuda,T.; Boulon,G. J. crystal growth. **2006**, 293, 517.
21. Davey,R.J.; Mullin,J.W. J. crystal growth. **1974**, 26, 45.
22. Yumashe,K.V.; Appl. Opt. **1999**, 38, 6343.
23. Natasha, A. N.; Sopyan, I.; Mel, M.; Ramesh, S. Med. J Malaysia. **2008**, 63, 85- 86.
24. Cheng, J. J.; Wu, J. M. Mater. chem. phys. **1999**, 48, 129.
25. Xiandong Wang.; Zhenquan Liu.; Andra Ambrosini.; Antoine Maignan.; Charlotte L. Stern.; Kenneth R. Poepelmeier.; Vinayak P. Dravid. Solid State Sciences. **2000**, 2, 99-107.
26. Santos,D.A.A.; Rocha,A.D.P.; Duque,J.G.S.; Macedo,M.A. J. Physics. **2010**, Conference series 200 IOP Publishing Ltd.
27. Bhagavannarayana,G.; Kushwaha,S.K.; Parthiban,S.; Subbaih Meenakshisundaram. J. crystal growth, **2009**, 311, 960- 965.
28. Kurtz,S.K.; Perry,T.T. J.Appl.Phys. **1968**, 39, 3798.
29. Banwell,C.N.; Mccash,E.M. Fundamentals of molecular spectroscopy; Fourth Eds; McGraw-Hill; Newyork, **1994**.
30. Kasthuri,L.; Bhagavannarayana,G.; Parthiban,S.; Ramasamy,G.; Muthu,K.; Subbiah Meenakshisundaram. Cryst.Eng.Comm. **2010**, 12, 493.
31. Balu,T.; Rajasekaran,T.R.; Murugakoothan,P. Current Applied Physics. **2009**, 9, 435-440.